Disposition of Azole Antifungal Agents. II. Hepatic Binding and Clearance of Dichlorophenyl-Bis-triazolylpropanol (DTP) in the Rat

Helen L. Bomont,[1,3] Michael H. Tarbit,[2,4] Michael J. Humphrey,[2] and J. Brian Houston[1,5]

Received December 6, 1993; accepted February 16, 1994.

DTP (dichlorophenyl-bis-triazolylpropanol) was evaluated as a probe of drug-cytochromes P450 interactions *in vitro* and *in vivo*. Studies with rat liver microsomes demonstrate that DTP shows similar P450 binding affinity to its analog, ketoconazole, as determined by P450 difference spectra and inhibition of the metabolism of methoxycoumarin. As a more polar azole, DTP shows less affinity for rat plasma albumin (fraction unbound 0.56) than ketoconazole (fraction unbound 0.037). DTP metabolism is simpler than that of ketoconazole, with only one pathway, N-dealkylation which removes a triazole ring to yield DTP glycol. This primary metabolite is further metabolised to a carboxylic acid, a glycol glucuronide and a third unknown secondary metabolite (probably an acid glucuronide). Over a dose range of 0.1-24mg/kg there is complete mass balance recovery in urine via the five metabolites and unchanged drug. However DTP metabolism is dose dependent and while the affinity of DTP for the cytochromes P450 carrying out the initial dealkylation is high (1.5μM based on unbound blood concentration), the capacity of the reaction is low (1nmole/min). Under linear conditions, metabolic clearance is low (19ml/h), but ten-fold higher than renal clearance. The liver is the major distribution site for both DTP and ketoconazole. At low DTP concentrations, a specific high affinity process dominates the hepatic binding of DTP resulting in a liver:blood partition coefficient of approximately 30. Hepatic binding is concentration dependent and the progressive decrease in partition coefficient observed as the dose of DTP is escalated is coincident with a decrease in volume of distribution. The two saturable processes involved in the disposition of DTP result in an unusual concentration dependency in the blood concentration-time profile of this azole. Following administration of a high dose (10mg/kg) of DTP the log concentration-time profile is sigmoidal. At high concentrations (above 1mg/L) both the N-dealkylation and the hepatic binding of DTP are saturated, but as concentrations fall to approximately 0.05mg/L the former process becomes linear and the time profile is convex over this concentration range. At later times as DTP concentrations decline further, the tissue binding also reaches the linear region and the time profile becomes concave. Only at low concentrations (below 0.05mg/L) do both processes become first order and the true half life is evident.

KEY WORDS: azole probes; nonlinear clearance; nonlinear liver binding; cytochrome P450 interactions.

[1] Department of Pharmacy, University of Manchester, Manchester, M13 9PL, UK
[2] Department of Drug Metabolism, Pfizer Central Research, Sandwich, Kent, UK
[3] Present address: Proctor and Gamble, Slough, Berkshire, UK
[4] Present address: Department of Drug Metabolism, Glaxo Group Research, Ware, Hertfordshire, UK
[5] To whom correspondence should be addressed

INTRODUCTION

Azole antifungal drugs inhibit cytochrome P450 51A1, the enzyme responsible for the 14α-demethylation of lanosterol to form the essential fungal membrane component ergosterol (1,2). Binding of substituted azoles to this hemoprotein is bimodal, and this characteristic contributes markedly to the effectiveness of these inhibitors (3). One mode involves direct co-ordination of a heterocyclic nitrogen atom (in the imidazole or triazole ring) with the heme iron and the second mode involves interaction between the lipophilic substituent and the apoprotein in the region of the substrate binding site. The early azole antifungals (ketoconazole, miconazole and clotrimazole) interact strongly with several mammalian cytochromes P450 in addition to the fungal P450 51A1(4–10). As a result these compounds have proven valuable in elucidating properties of P450.

We have recently detailed the *in vivo* disposition of ketoconazole in the rat (11). Ketoconazole-P450 interactions are reflected not only in its clearance but also in its hepatic binding which affects its volume of distribution. The complex *in vivo* disposition of ketoconazole accounts for inconsistencies observed between *in vitro* and *in vivo* inhibitory potency studies. These investigations also highlight the potential of azole antifungals as probes of the P450 superfamily. However, ketoconazole has properties that limit its usefulness as a molecular probe: a) strong affinity for proteins (as exemplified by its avid binding to plasma albumin) which may confound the cytochrome P450 interactions (11); b) formation of several metabolites via parallel pathways which is indicative of multiple P450 involvement (12); and c) formation of unknown ketoconazole metabolites.

The studies described herewith focus on another azole compound-dichlorophenyl-bis-triazolylpropanol (DTP—Fig. 1). This triazole has strong affinity for both fungal and mammalian steroidogenic P450s, and this lack of selectivity limits the clinical value of this compound as a candidate for antifungal therapy. We have investigated in the rat a) whether the hepatic binding phenomenon reported for ketoconazole occurs with other azoles, namely DTP, and b) the metabolic fate and disposition characteristics of DTP. The general findings of these studies illustrate that drug interactions with cytochrome P450 can lead to complex nonlinear kinetics *in vivo* involving both distribution as well as elimination processes.

MATERIALS AND METHODS

Metabolite Excretion Studies Twenty-four hours prior to dosing, male Sprague-Dawley rats (240-250g, n = 20) were placed in individual metabolism cages for the collection of control urine and faeces, and to acclimatize the animals to the imposed conditions. These animals were divided into five dosage groups and a single intra-peritoneal (ip) dose of ^{14}C-DTP (2-10μCi/kg; 0.1, 0.5, 1, 10 or 24 mg/kg in propylene glycol (PG): saline 0.9%, 3:7, 10ml/kg), was administered to each rat, and excreta samples collected every twelve hours over a six day period. ^{14}C-DTP was analysed in the urine by a selective radiochemical assay (see below). Total radioactivity was determined in the faeces by a sample oxidation

0724-8741/94/0700-0951$07.00/0

technique in conjunction with liquid scintillation counting. Urinary drug related components were separated and quantitated by radio-TLC, and identified by co-chromatography of authentic standards overlaid in urine.

Aliquots of undiluted urine (120μl) were applied to a silica gel TLC plate (Merck F_{254}, 0.25mm) which was developed with chloroform:methanol:ammonia (80:20:1v/v/v). The radiolabelled compounds were detected and quantitated by scanning the plate with a linear plate analyser (Isomess IM 300 in conjunction with the Isomess IM 3000 software package). The relative amount of each of the six radiolabelled drug related components, on the chromatogram, was determined by analysis of the area under the curve of each discrete band on the trace. The radioactive content of each component was expressed as a percentage of the total area. Autoradiography was used to verify that the radiolabelled components were separated into discrete bands. The TLC plate was placed in direct contact with X-ray film in a polythene bag which was sealed under vacuum and stored at −20°C. After approximately fourteen days, the autoradiogram was produced by developing the X-ray film.

Prior to enzymatic hydrolysis, an aliquot of neat urine (3-5ml, known radioactive content) was passed slowly through an XAD-2 resin column (12cm × 1 cm, in the aqueous phase), followed by distilled water (60 ml). The aqueous eluate was collected and retained. After drying the column with hexane (40ml), an aliquot of methanol (60ml) was passed through and the eluate collected. The radioactive content was quantitated in each eluate (100μl) by liquid scintillation counting, and the remaining aqueous fraction was freeze-dried and store at −20°C. The methanolic solution was evaporated to dryness under nitrogen at 37°C and stored at −20°C. The methanolic residue was reconstituted in methanol (400μl) and incubated, at 37°C for sixteen hours, with β-glucuronidase (Type B1, 100,000 units, 1ml) and acetate buffer (0.1M, pH5, 1ml). The reaction mixture was then freeze-dried, the resultant powder constituted in methanol and transferred to a clean tube. The sample was evaporated to dryness under nitrogen at 37°C, again reconstituted in methanol, centrifuged at 3,000rpm for five minutes and pipetted into a clean tube. This procedure was repeated until the sample was clean. The final residue was reconstituted in methanol (150μl), and chromatographically analysed.

Blood Concentration-time Profiles and Clearance Determination A second set of male Sprague-Dawley rats (240–260g, n = 20) were placed in metabolism cages twenty-four hours prior to dosing, for the collection of control urine, and to acclimatize the animals to the imposed conditions. Five dosage groups were assigned and a single ip dose of ^{14}C-DTP (2-10μCi/kg; 0.1, 0.5, 1, 10 or 24mg/kg in PG/saline 0.9%, 3:7; 10ml/kg) was administered to each rat. Blood samples (n = 8–11, 200–500μl) were taken via the tail artery over an 80 hour period. Urine samples were collected, every 12 hours, from 0 to 72 hours after dosing. On completion of the 80 hour blood sample, the rats were killed by cervical dislocation and their bladders emptied to ensure a complete urine collection. ^{14}C-DTP was quantitated, in both blood and urine, by the radiochemical assay detailed below.

An extended time course study was performed which involved the administration of a single ip dose of ^{14}C-DTP (240μCi/kg; 10mg/kg in PG/saline 0.9%, 3:7; 10ml/kg) to male Sprague-Dawley rats (210–230g, n = 4) and subsequent blood sampling (n = 14–16, 150–500μl), via the tail artery, over a 250 hour period. The analysis of DTP was carried out as above.

The apparent volume of distribution for DTP was determined by dividing the dose by the blood concentration at time zero. Area under the blood concentration-time curve (AUC) was calculated by the trapezoidal rule and total body clearance by dividing dose by AUC.

Urinary excretion rate-time plots for DTP and its metabolites showed parallel behaviour indicating the metabolite kinetics were formation rate limited (13). Therefore excretion rate of metabolites were taken as a good measure of formation rate and metabolic clearance (CLm) calculated from eq 1 using the blood concentration of DTP at the midpoint of the urine collection interval (C_{mid})

$$CL_m = \frac{\text{Excretion rate of metabolites}}{C_{mid}} \quad (1)$$

Renal clearance (CL_R) of DTP was calculated by the analogous equation -

$$CL_R = \frac{\text{Excretion rate of DTP}}{C_{mid}} \quad (2)$$

Determination of Blood to Plasma Concentration Ratio An aliquot of ^{14}C-DTP (0.001–0.15μCi/ml, 0.01–100 mg/L, in methanol) was transferred to a glass tube and evaporated to dryness under nitrogen prior to addition of fresh blood (2.2 ml). The samples were equilibrated at 37°C, in a shaking waterbath, and an aliquot of the spiked blood (200μl) removed for total radioactive counting. The remaining sample was centrifuged at 3,000rpm, 37°C for five minutes and an aliquot of plasma (100–200μl) taken for quantitation of ^{14}C-DTP by liquid scintillation counting. The blood:plasma ratio was calculated from the radioactivity per ml of blood and plasma respectively.

Determination of Plasma Protein Binding Fresh blank plasma (2ml) was spiked with ^{14}C-DTP (0.001–0.15μCi/ml, 0.01–100mg/L), and an aliquot (200μl) taken for quantitation of radioactivity and a known volume (1.6ml) pipetted into a polyallomer ultracentrifuge tube. Centrifugation (180,000g) was carried out under vacuum at 37°C for fifteen hours (Sorvall Ultracentrifuge Model OTD 65D). The centrifuge was stopped without breaking, to minimize turbulence, and an aliquot (100–200μl) was sampled from the plasma water via a needle and syringe. The sample was analysed for ^{14}C-DTP by liquid scintillation counting. The fractions unbound (fu) was calculated from the ratio of the radioactivity per ml of plasma water and the radioactivity per ml of total plasma.

Tissue Binding Determination A fourth set of male Sprague-Dawley rats (240–260g, n = 25) received a single ip dose of ^{14}C-DTP (2–10μCi/kg; 0.1, 0.5, 1, 10 or 24 mg/kg in PG/saline 0.9%, 3:7; 10ml/kg). Twenty-four hours after ^{14}C-DTP administration, blood was sampled by cardiac puncture and the liver, kidneys and lungs removed, weighed and homogenized in SET buffer (0.25M sucrose, 20mM tris-(hydroxymethyl)aminomethane base, 5.4mM ethylenediamine tetraacetic acid; pH 7.4; 10ml liver, 5 ml kidney, 3ml lung) at 4°C. The resultant tissue homogenates were stored in 1ml Eppendorf vials at −70°C. Analysis of DTP, in both

blood and homogenate samples, was performed using the radiochemical assay procedure.

Tissue: blood partition coefficients (Kp) were determined from the ratio of the radioactivity per g of tissue to the radioactivity per ml of blood. To account for metabolism within a tissue, the Kp calculation should incorporate a correction factor based on its clearance (14). DTP is a low clearance drug, and its hepatic extraction ratio is extremely low (< 1%). Thus, although the liver is the major eliminating organ, the Kp value per liver was not corrected for metabolism.

Unbound fractions for tissues (fu_T) were derived from partition coefficients and blood unbound fractions (15)-

$$fu_T = fu_b/Kp \quad (3)$$

Radiochemical Assay for DTP This radiolabelled assay is selective for the analysis of DTP in whole blood, urine and tissue homogenates. All glassware was silanized; clean glassware was immersed in a solution of dichlorodimethylsilane (2%) in toluene for twenty-four hours, rinsed in methanol and then in distilled water.

Total radioactive content in each sample was determined by liquid scintillation counting prior to extraction of DTP. An aliquot of either blood (0.1–1 ml), urine (1 ml) or tissue homogenate (1ml) was extracted into chloroform (5ml) by rotary mixing for ten minutes. The two phases were separated by centrifugation, and the aqueous layer removed by aspiration. An aliquot of chloroform layer (200μl) was transferred to a scintillation vial, and the amount of ^{14}C-DTP quantitated by liquid scintillation counting. The extraction procedure was scaled up for samples with a low radioactive content. After extraction the separated chloroform layer was transferred to a scintillation vial and evaporated to dryness under nitrogen at 37°C. The residue was reconstituted in scintillant. Duplicate extractions were performed for each sample, and a range of ^{14}C-DTP standards were extracted and quantitated concurrently to determine the extraction efficiency for each separate run. The extraction efficiency in blood and urine was greater than 92%, whereas in liver homogenates the efficiency was 87%. The calculation used to determine the DTP concentration included a correction factor to account for extraction efficiency. This radiochemical assay for DTP was validated by radio-TLC. Only the parent drug was extracted into the organic layer; all metabolites remained in the aqueous phase.

Determination of Substrate Binding to Cytochromes P450 Binding difference spectra in rat hepatic microsomes were measured based on the spectrophotometric titration method of Schenkman(16). Diluted microsomes (1nmole cytochrome P450/ml in phosphate buffer 0.1M,pH 7.4; 2ml) obtained by standard methodology from untreated rats were used. Stock solutions of azoles were prepared in dimethylsulphoxide (DTP) or dimethylformamide (ketoconazole) and aliquots were mixed with microsomes, a three minute equilibration allowed, and the difference spectrum recorded between 500 and 360nm (Pye-Unicam Spectrophotometer SP8-500) at 37°. Equivalent values of solvent were added to the reference cuvette. The final concentration of organic solvent never exceeded 1%, and each measurement was carried out in triplicate. The absorbance peak minus trough values were used to construct an Eadie-Hofstee plot from which, the maximum absorbance change (Amax) and the spectral dissociation constant (Ks) were calculated.

Methoxycoumarin O-demethylase (MCOD) activity was determined by a fluorometric assay which continuously and directly monitored the formation of the product 7-hydroxycoumarin (17). Inhibitor constants (K_Is) were determined from Dixon plots of data obtained at three substrate concentrations (0.1, 0.3, 1mM) and nine azole concentrations (0.5–500μM). Basal rates were determined in the presence of identical volumes of solvent (1–10μl) to the inhibitor studies.

Chemicals The following were supplied by Pfizer Central Research (Sandwich, Kent, UK)—2-(2,4-dichlorophenyl)-1, 3-bis(1H-1,2,4-triazol-l-yl)-propan-2-ol (DTP), [^{14}C-triazole]—DTP (61.8μCi/μmole, radiochemical purity > 99%), DTP-diol, DTP-carboxylic acid, triazole and ketoconazole.

RESULTS

Azole-cytochromes P450 interactions in vitro Titration of hepatic microsomes, with either DTP or ketoconazole, resulted in type II spectral interactions which were characterized by peak, isobestic and trough wavelengths of 429, 418, 396nm and 428, 416, 394nm respectively. Both DTP and ketoconazole bind to hepatic microsomal cytochromes P450 in the classical nonlinear fashion and when the data (the absorbance difference between peak and trough values) were analysed using the Eadie-Hofstee approach it was evident, that more than one binding site existed for both DTP and ketoconazole. The model that was found to fit the data best resolved the binding into two integral saturable components; a high affinity and a low affinity binding site. Table I shows that comparable affinity is demonstrated by both azoles with dissociation constants for the high affinity sites below 1μM.

DTP and ketoconazole were both found to inhibit the cytochromes P450-mediated methoxycoumarin O-demethylation reaction. Biphasic Dixon plots were observed for both azoles. Apparent K_Is were estimated from the initial linear phase (0.2–10μM azole) and found to be 3.5 and 9.8 μM for ketoconazole and DTP, respectively.

Metabolic fate of DTP Over the DTP dose range studied (0.1–24mg/kg), no dose dependency was observed in the

Table I. Comparison of DTP and ketoconazole interactions with cytochromes P450.[a]

	DTP	Ketoconazole
Ks_1 (μM)	0.17±0.02	0.063±0.004
Absorption max_1 (OD units/nmole P450)	0.016±0.001	0.009±0.008
Ks_2 (μM)	8.7±0.8	3.6±0.3
Absorption max_2 (OD units/nmole P450)	0.056±0.007	0.062±0.006
K_I (μM)	9.8	3.5

[a] Spectral data are the mean ± sd of determinations with 5 microsomal preparations. 1 and 2 refer to high and low affinity sites. Inhibition constant determined with respect to methoxycoumarin at 3 substrate concentrations (0.1–1mM) and at least 6 inhibition concentrations (1–1000μM)

percentage of radioactive dose excreted in the urine (range 73–80%) and faeces (range 9–11%), or in the volume of urine produced (range 74–83ml) over the experimental period of 144 h. Since the major route of excretion for DTP and metabolites is via the urine, subsequent metabolite identification was confined to the urine. Radiochromatograms of pooled urine after administration of various doses were qualitatively identical with six drug related components which, with autoradiography, were all confirmed to be discrete bands. Initial characterization was carried out by co-chromatography of authentic standards added to urine which identified DTP, triazole and carboxylic acid and diol derivatives of DTP.

To characterize any drug related conjugates, the urine was treated with β-glucuronidase which resulted in the disappearance of one component and an increase in the area under the chromatogram of the diol metabolite. Thus a fifth metabolite was identified as the diol glucuronide. Following the isolation of each component, by scraping the relevant areas of the TLC plate, absolute identification was carried out with mass spectrometry. (Data on file, Pfizer Central Research, Sandwich). The sixth component remains unidentified. This metabolite did not co-chromatograph with the aldehyde or primary amine derivative of DTP, nor did it undergo enzymatic hydrolysis with β-glucuronidase. Thus the azole DTP is either excreted unchanged in the urine, or undergoes an oxidation reaction in which one molecule of parent drug is N-dealkylated to yield one triazole and one diol entity. The triazole entity is excreted in the urine without further metabolism, whereas the diol moiety is either directly excreted, or glucuronidated, or oxidised to form the carboxylic acid metabolite (see Fig. 1). From mass balance considerations, the unknown metabolite must be formed from a metabolic reaction sequential to the formation of the triazole and diol moieties, and hence this eliminates the possibility of a direct conjugation of the parent drug. It is postulated that the unknown component is formed from a conjugation reaction involving the carboxylic acid metabolite.

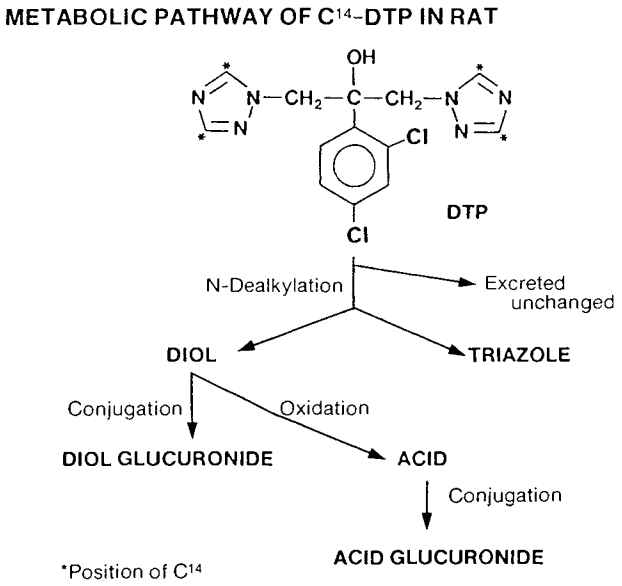

Figure 1. Metabolic pathway of ^{14}C-DTP in the rat. * shows position of radiolabel.

Dose dependency was observed in the relative amounts of parent drug and metabolites excreted in the urine (Table II). As the dose was increased from 0.1mg/kg to 24mg/kg, the fraction excreted unchanged in the urine increased by almost 3 fold, from 0.19 to 0.55, and the total fraction metabolized decreased accordingly from 0.83 to 0.45. The urinary elimination of the triazole, unknown and acid metabolites displayed a dose dependency, with the amount of each metabolite decreasing by approximately 50% over the dose range studied. In contrast, the diol and diol glucuronide were excreted in a dose independent fashion. The diol is an intermediate metabolite, and is therefore not a sensitive parameter of dose dependency. The linearity observed in the diol glucuronide may reflect that the glucuronyltransferase involved in the formation of this metabolite has a higher affinity for the diol than the oxidase system producing the acid metabolite, and is consequently the favoured metabolic route.

Binding within the blood matrix Over the 10,000 fold DTP concentration range studied (0.01–100mg/l), the blood to plasma ratio was calculated to be approximately one (range 0.98–1.02 for the six concentrations studied, largest coefficient of variation 3%). This reflects that DTP does not bind extensively to erythrocytes, but is associated mainly with the erythrocyte water.

No significant (one way ANOVA) concentration dependent nonlinearity was evident in the binding of DTP to plasma proteins over the concentration range studied (0.01–100mg/l). Approximately 44% of DTP was bound to plasma proteins (range 42.7–44.4% for the six concentrations studied, largest coefficient of variation 3.4%) reflecting a low degree of vascular binding, and hence the unbound fraction in whole blood is 0.56.

Blood Concentration-Time Profiles A typical log blood concentration-time profile, for each of the DTP dose investigated, is depicted in Fig. 2. From these time profiles it is evident, that both the intercepts and the area under the curve (AUC) show a disproportionate increase with escalating dose. Mean data for the calculated pharmacokinetic parameters, volume of distribution (V), total clearance (0–80hr) and half-time are shown in Table III.

Over the 240 fold dose range studied, the V term displayed nonlinear behaviour. This distribution parameter was calculated from the concentration intercepts by extrapolation to time zero which did not pose a problem because the absorption phase was very rapid and essentially complete (see earlier) and the decline regular. As the dose increased from 0.1 to 24mg/kg, the V decreased, by almost half, from 661 to 364m./SRW. The standard rat weight (SRW) in these experiments was 275g. The observed trend in V can be explained by the saturation of DTP tissue binding sites at high concentrations.

The calculation of clearance (CL) however is more problematic due to the characteristics exhibited by concentration-time profiles. From the calculated AUC_{0-80} it is evident that the apparent clearance over the study period (CL_{0-80}) was nonlinear, decreasing by 66% from 27 to 9 ml/hr/SRW with increasing dose. True estimates of CL could not be calculated as the nonlinear behaviour prevents extrapolation of the blood concentration-time profile.

Similarly, the nonlinearities prevent the calculation of a

Table II. Effect of dose administered of DTP on urinary excretion products

Drug related component (Rf value)	% of Recovered ^{14}C following administration of DTP				
	0.1mg/kg	0.5mg/kg	1.0mg/kg	10.0mg/kg	24.0mg/kg
DTP (0.75)	18.5 ± 0.5	17.7 ± 0.4	25.2 ± 1.2[c]	39.9 ± 1.7[c]	54.5 ± 1.4[c]
Triazole (0.48)	41.1 ± 0.6	41.4 ± 0.5	37.3 ± 0.9[b]	29.7 ± 1.1[c]	22.8 ± 0.9[c]
"Total diols"	41.9 ± 0.5	41.2 ± 0.2	37.6 ± 1.7[a]	30.8 ± 4.3[c]	22.7 ± 2.2
Diol (0.57)	2.8 ± 0.7	3.2 ± 0.4	4.8 ± 1.15	2.9 ± 0.5	2.4[c] ± 0.4
Acid (0.37)	10.8 ± 0.8	9.8 ± 0.6	7.7 ± 0.8[b]	7.4 ± 0.9[b]	5.6 ± 0.8[c]
Unknown (0.29)	19.8 ± 0.7	19.6 ± 0.6	15.9 ± 0.8[c]	12.1 ± 0.8[c]	8.0 ± 0.5[c]
Diol glucuronide (0.20)	8.6 ± 0.6	8.6 ± 0.6	9.2 ± 0.7	8.2 ± 0.7	7.7 ± 0.5

Results are presented as mean ± S.D.; n= 4
"Total diols" are the sum of Diol, Acid, Unknown and Diol glucuronide
Statistically different from DTP 0.1 mg/kg; (one way ANOVA with means contrasted) [a] $p < 0.05$, [b] $p < 0.01$, [c] $p < 0.001$.

meaningful elimination t½, and thus the half-time, a parameter which represents the slope over the study period, was calculated. Due to the degree of saturation evident at the higher DTP doses, half-time was calculated from data gathered in the later phase of the experiment. Over the DTP dose range studied it is apparent that the elimination of this azole from the blood occurred in three distinct phases; a slow elimination phase (at blood concentration above 1mg/L), a more rapid phase (at concentrations 0.05-1mg/L) and an apparent linear phase (at concentrations below 0.05mg/L). The characteristic trend observed in the half-time is a direct consequence of the nonlinear V and CL. The initial reduction in half-time, with increasing dose, may be attributed to the decrease in V, whilst the final increase may be explained by the change in CL.

Clearance Processes To examine the nonlinear elimination of DTP in more detail the two mechanisms of clearance, renal and metabolic, were separated. By relating the urinary excretion rate of DTP or metabolites to the blood DTP concentration, renal and metabolic clearance respectively can be estimated. When the two mechanisms of DTP clearance are divorced it is evident that the renal clearance is linear, whereas nonlinear behaviour is apparent in the metabolic clearance (Fig. 3). As the blood DTP concentration increased from 0.005 to 12mg/l, the metabolic clearance decreased dramatically, from 25 to 0.2ml/h/SRW, indicating that at high DTP concentrations metabolism becomes satu-

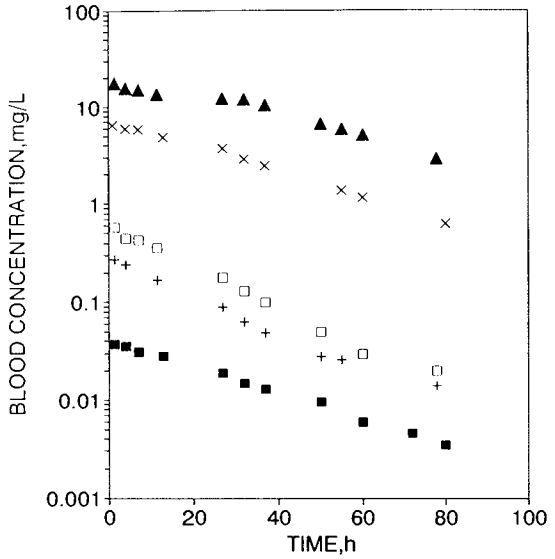

Figure 2. Blood concentration-time profiles for DTP following bolus administration. Doses administered i.p. at 0.1 (■), 0.5 (+), 1 (□), 10 (×) and 24(▲)

Table III. Effect of dose of DTP on blood concentration-time profiles.

DTP dose (mg/kg)	Pharmacokinetic parameter		
	Volume of distribution (ml/SRW)	$Clearance_{0.80}$ (ml/hr/SRW)	Half-time (hr)
0.1	661 ± 21	24.0 ± 1.8	20.4 ± 1.4
0.5	547 ± 24[a]	26.9 ± 2.0	13.4 ± 0.6[a]
1.0	458 ± 14[a]	25.5 ± 5.0	13.3 ± 1.2[a]
10.0	397 ± 7[a]	10.9 ± 0.4[a]	23.2 ± 3.2
24.0	364 ± 18[a]	9.1 ± 0.9[a]	23.5 ± 1.9

Results are presented as mean ± S.D.; n=4
Statistically significant from single dose DTP 0.1mg/kg (one way ANOVA with means contrasted) [a] $p < 0.001$

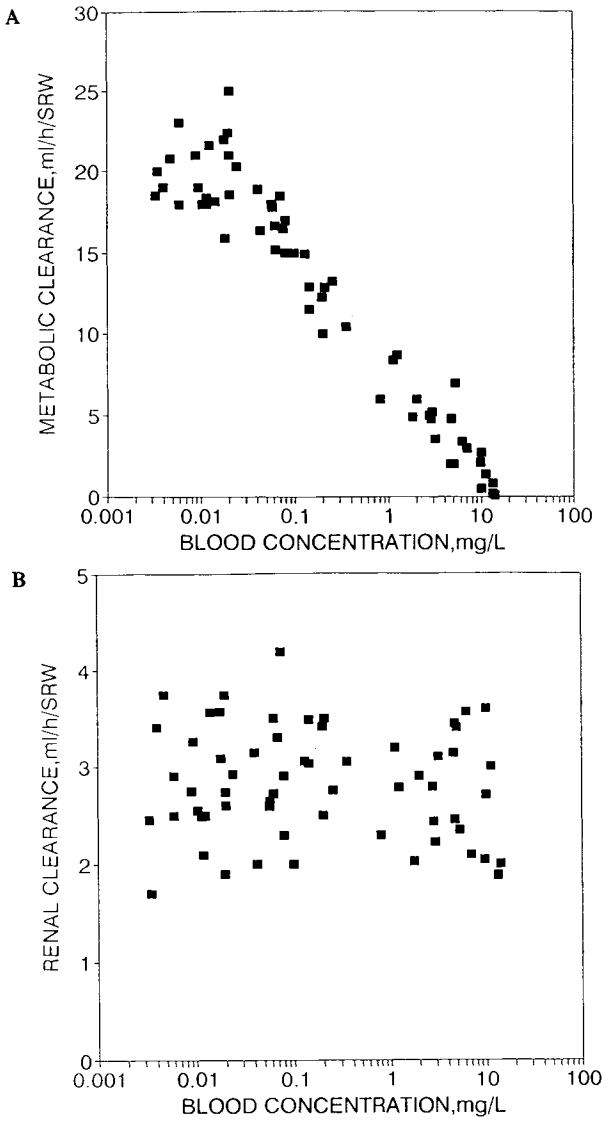

Figure 3. Relationship between (A) metabolic clearance and blood concentration of DTP and (B) renal clearance and blood concentration of DTP. Data shown for 5 doses and 20 individual animals.

rated. Using a Michaelis-Menten type kinetic model (see Table IV), nonlinear regression gave parameter estimates of 51.6nmol/h/SRW for Vmax and 2.7μM for Km. When expressed in terms of unbound blood concentration Km reduced to 1.5μM.

Analysis of the renal clearance data provides an average value of 2.79ml/h/SRW and when corrected for blood binding the renal clearance increases to 5ml/h/SRW. When compared to the glomerular filtration rate in the rat (132ml/h/SRW, ref. 18), these data are indicative of an extensive tubular reabsorption process for DTP, which is not surprising since this triazole is a relatively small, lipophilic molecule.

Tissue Binding In order to assess the relative tissue and plasma binding of DTP, partition coefficients (Kp) between total drug concentrations in liver (Kp_H), kidney (Kp_K) and lung (Kp_L) and total drug concentration in blood were determined (see Table V). Over the wide blood concentration range covered (0.018–10mg/l), the kidney and liver both possessed a greater affinity for DTP, than the blood. In contrast, the concentration of DTP in the lung was not significantly different from that in the blood, resulting in Kp_L values of approximately one. No significant relationship (one way ANOVA) was observed between either Kp_L or Kp_K and DTP blood concentration.

In contrast to pulmonary and renal distribution, hepatic distribution of this azole clearly deviates from linearity (see Fig. 4). At the lowest blood concentration (0.018mg/l), the total concentration of DTP per ml (g) liver was greater than 29 times that of the blood. The relatively high Kp_H value reveals that the liver has an extremely high affinity for DTP in relation to the blood, kidney and lung. These data, indicating extensive binding process(es) in hepatic tissue, are compatible with the high binding affinity constant of DTP for hepatic microsomal cytochromes P450 observed spectrally. Over the DTP concentration range of 0.018 to 10mg/l, the Kp_H decreased 6.5-fold.

Table V also lists the parameter Kp_{REST} which represents partitioning into a fictitious average tissue of distribution. It is calculated by the equation shown in Table V by subtracting the contribution of hepatic distribution from the overall volume of distribution of DTP. Kp_{REST} shows no concentration dependence which would suggest that saturation of liver binding is the main event governing the observed reduction in V over the dose range studied.

From Kp and fu_b, the fraction unbound in the tissue can be calculated (Eq 3). For the kidney and lung the unbound fractions are constant, over the 1,000-fold concentration range studied, at 0.25 and 0.5 respectively. For liver where the high Kp results from extensive liver binding the fu_H is very low and concentration dependent (Fig. 4). The fu_H is 0.019 at the lowest DTP blood concentration studied and increased, by approximately 6 fold, to 0.125. These hepatic data reflect a saturation of binding sites within the liver which contrasts with the linear fu_b over the same concentration range.

When the binding data were plotted using the conventional Eadie-Hofstee approach it was evident that more than one binding site existed. The model that fits the data best resolved the binding into two integral components; a saturable and nonsaturable process. The data were analysed using a model analogous to the Michaelis-Menten equation with a linear component (22)

$$Cb = \frac{Bmax \cdot Cu}{Kd + Cu} + B_2 \cdot Cu \qquad (4)$$

where Cb and Cu are the bound and unbound hepatic tissue concentrations, Bmax and Kd are the maximum capacity of and dissociation constant for a high affinity, low capacity binding site and B_2 is the binding coefficient for a low affinity, apparently unlimited capacity binding site. The maximum capacity of the saturable binding component was calculated to be 12nmoles DTP/g liver, and the binding affinity dissociation constant was determined to be 0.24μM. For comparative purposes the binding coefficient for the high affinity site (B_1) can be calculated from the ratio of Bmax and Kd. At low DTP concentrations, the saturable liver binding component is approximately 7 times more important than the linear process as reflected in the binding coefficient val-

Table IV. Kinetic parameters describing the elimination of DTP

Pharmacokinetic parameter	Total concentration	Unbound concentration
METABOLIC CLEARANCE[a]		
Vmax (nmol/hr/SRW)	51.6	51.6
Km (μM)	2.7	1.5
(mg/l)	0.9	0.5
Intrinsic Clearance (ml/hr/SRW)	19.2	34.2
RENAL CLEARANCE (ml/hr/SRW)	2.8	4.9

[a] The Michaelis-Menten parameters were obtained by fitting the equation - Rate of metabolism = Vmax·C/Km + C where C was the observed mid-point blood concentration for the time interval over which the rate was measured. See Materials and Method section.

ues of 50 and 7ml/g for saturable and linear binding processes respectively.

DISCUSSION

Azoles are useful *in vitro* probes of cytochromes P450. Numerous spectral and inhibitory studies have been performed with a variety of microsomes (for example, 4-10, 24) and purified enzymes (19,20). Also, X-ray crystallography has been employed to investigate the topography of the active site of $P450_{cam}$ with this class of compounds (21). Ketoconazole has become the prototype for azole-P450 investigations *in vitro*. However, several inconsistencies exist for the behaviour of this compound *in vitro* and *in vivo* (11). Much of this anomaly may be a consequence of the pharmacokinetics of ketoconazole. Both the volume of distribution and clearance of this azole are dose dependent (11). The former is due to saturable hepatic binding which can be resolved from its hepatic clearance which is also saturable. Although these phenomena are not unprecedented (for example they also occur with some coumarins—22,23), they are of particular interest for azoles in view of their unusually strong affinity for P450.

Table V. Tissue-blood partition coefficients for DTP.

Dose (mg/kg)	Blood concentration (mg/L)	Kp_H	Kp_K	Kp_L	Kp_{REST}
0.1	0.018 ± 0.002	29.4 ± 1.2	2.4 ± 0.2	1.2 ± 0.1	2.4
0.5	0.098 ± 0.026	23.4 ± 0.1[a]	2.1 ± 0.2	1.0 ± 0.1	2.0
1.0	0.22 ± 0.040	15.1 ± 1.1[a]	2.2 ± 0.2	1.2 ± 0.2	2.2
10.0	4.1 ± 0.2	6.2 ± 0.5[a]	2.3 ± 0.1	1.2 ± 0.1	2.3
24.0	9.9 ± 0.5	4.5 ± 0.5[a]	2.1 ± 0.2	1.1 ± 0.1	2.4

Results are presented as mean ± S.D.; n = 5
Statistically significant from DTP 0.1mg/kg (one way ANOVA with means contrasted) [a] $p < 0.01$
Kp_H, Kp_K and Kp_L refer to the hepatic, kidney and lung tissue: blood partition coefficients, respectively.
Kp_{REST} represents an average tissue partition coefficient calculated from re-arrangement of eq. 6 $Kp_{REST} = (V - (V_b + Kp_H \cdot V_H)/V_{REST}$

DTP is more polar than ketoconazole, Log P values of 1.1 and 3.9, respectively (24). DTP and other triazoles bind strongly to P450s, similar to imidazoles in mouse (26) and rat microsomes (this study). Both DTP and ketoconazole display classic Type II binding spectra which may be analysed in terms of two classes of binding sites with similar affinities and capacities for the two azoles. Both azoles give low μM K_I values for MCOD inhibition which are consistent with previously published K_I values for ketoconazole (5,7–10). In contrast to its strong affinity for P450, DTP shows only moderate interactions with plasma albumin (fraction unbound 0.56) over a wide concentration range. Ketoconazole binding to rat plasma albumin is also concentration independent but much more substantial—fraction unbound 0.037 (11).

Hepatic clearance of ketoconazole is entirely responsible for the elimination of this azole (12), and numerous metabolites are formed (20). In contrast, the elimination of the more polar azole DTP occurs by both renal and hepatic clearance. At low concentrations, metabolism is the most important eliminating process, whereas at the higher concentrations renal clearance becomes more significant because of saturation of the DTP N-dealkylation metabolic pathway. The fraction metabolised decreases from over 80% to less than 50% over the dose range studied. The preference for metabolism as an eliminating route can be seen in the ten-fold difference between the intrinsic metabolic clearance and the renal clearance (Table IV).

The metabolic fate of DTP is quite simple. An initial dealkylation removes a triazole ring to leave DTP glycol. The latter primary metabolite is further metabolised to yield a carboxylic acid, a glycol glucuronide and unknown metabolite we speculate is an acid glucuronide (see Fig. 1). Although the affinity of DTP for the P450s carrying out the initial dealkylation is high (1.5μM based on unbound plasma concentrations), the capacity for the reaction is low (1 nmole/min/SRW). Under linear conditions the metabolic clearance is 19ml/h/SRW which corresponds to a low hepatic extraction ratio of 0.014.

The liver is also the major distribution site of DTP. At low DTP concentrations, a specific high affinity binding process dominates the hepatic binding of DTP resulting in a Kp_H of approximately 30. At high DTP concentrations the

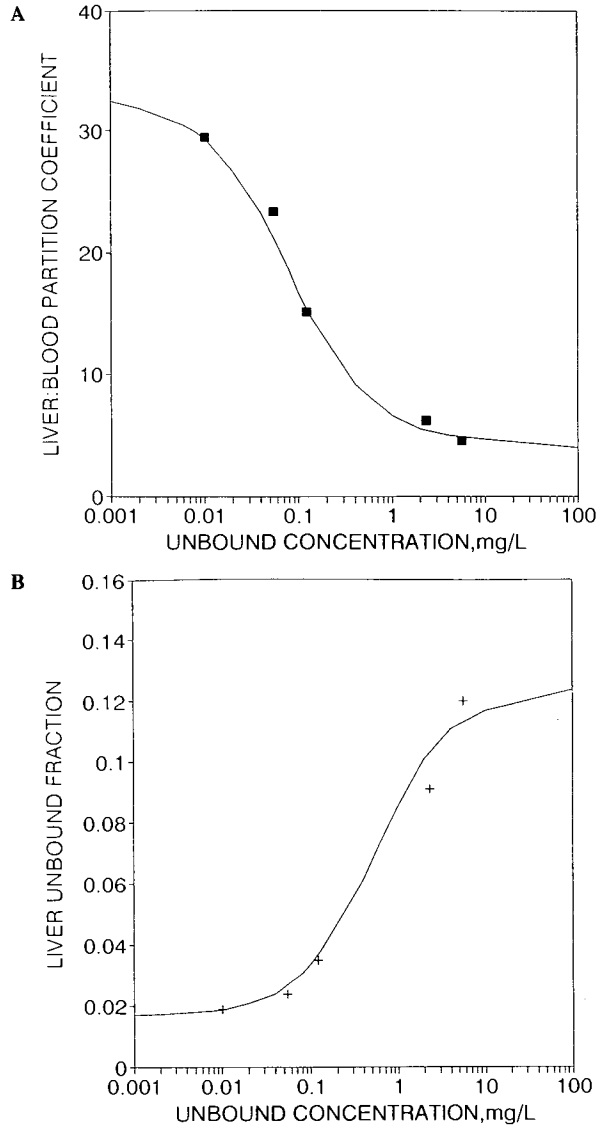

Figure 4. Relationship between (A) liver:blood partition coefficient and unbound DTP blood concentration and (B) fraction unbound in liver and unbound DTP blood concentration. Average values for each dose studied is shown. Lines refer to the predicted relationships using equations—

$$fu_H = \frac{Kd + Cu}{Kd + Bmax + Cu + (B_2 \cdot Kd) + (B_2 \cdot Cu)}$$

$$Kp_H = \frac{fu_b[Kd + Bmax + Cu + (B_2 \cdot Kd) + (B_2 \cdot Cu)]}{Kd + Cu}$$

and the parameter values given in the text.

high affinity site(s) saturate and a low affinity linear binding component becomes relatively more important and Kp_H falls to approximately 4. This value however still exceeds by at least two-fold the Kp of any other measured tissues, none of which show nonlinearity. At low concentrations the effective volume of distribution within the liver ($Kp_H \cdot V_H$ where V_H is the volume of liver—11ml/SRW) is 323ml/SRW which is approximately one half of the total volume of distribution. Similar calculations have been performed for ketoconazole (11) and the liver's contribution to the total volume of distribution for this azole was found to be one third. In the latter case data from steady-state experiments were used in determining Kp. For DTP we have used single bolus doses, however, in view of the slow elimination of this azole we are confident that tissue distribution equilibrium exists in these studies.

The progressive decrease in Kp_H observed as the dose of DTP is escalated is coincident with the decrease in V. Fig. 5 illustrates the strong relationship between these two parameters. This observation is in keeping with the physiological modelling approach to drug distribution (25,26) which is based on the general equation -

$$V = V_b + \Sigma Kp_{Ti} \cdot V_{Ti} \qquad (5)$$

where V_b and V_T are the volumes of blood (22ml/SRW) and other body water compartments (143ml/SRW) respectively, and the sum of these is total body water (165ml/SRW or 600ml/kg).

If the liver is isolated from the collective "tissue" term, then -

$$V = V_b + Kp_H \cdot V_H + Kp_{REST} \cdot V_{REST} \qquad (6)$$

where V_{REST} is now the sum of the body water compartments excluding blood and liver (132ml/SRW) and Kp_{REST}, an average tissue partition coefficient (See also Table V). Thus a plot of V against Kp_H should yield a slope of V_H (11ml/SRW) and an intercept equivalent to ($V_b + Kp_{REST} \cdot V_{REST}$). The slope from Fig. 5 is 10.98ml/SRW which is in excellent agreement with the mean liver weight (11g) recorded in these distribution studies. Consequently it can be concluded that the nonlinearity in the V term for DTP can be solely explained by hepatic binding.

The two saturable processes involved in the disposition

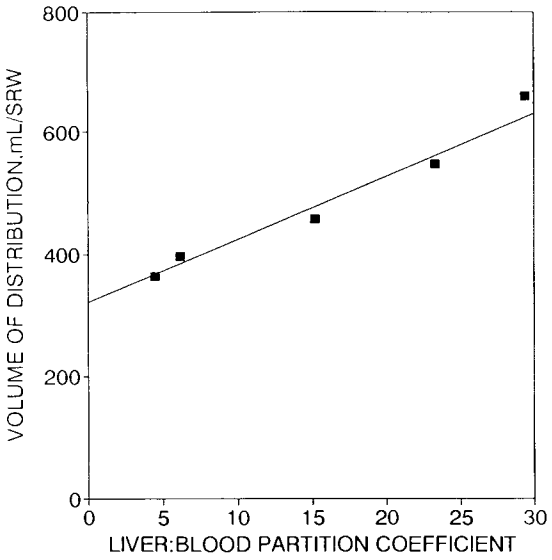

Figure 5. Relationship between volume of distribution and liver: blood partition coefficient for DTP. Each symbol represents a different dose of DTP. The theoretical relationship is discussed in the text and predicts the following

$$V = V_b + Kp_T \cdot V_T + Kp_H \cdot V_H$$

The values for the slope and intercept following linear regression (r = 0.984) are 10.98ml and 320ml, respectively.

of DTP affect the blood concentration-time profile. Under linear conditions, DTP is extensively metabolized via a single pathway and is extensively distributed to hepatic tissue. Hence, if the nonlinear kinetics of DTP are solely due to a saturable elimination process convex log concentration-time profiles should be evident (27). Conversely, if the dose dependency is only attributable to nonlinear tissue binding, then for a low clearance drug like DTP concave log concentration-time profiles should be apparent (28). However, two sources of nonlinearity occur in the disposition of DTP; capacity-limited metabolism and saturable hepatic binding. Based on the six-fold difference observed in the Km and Kd parameter estimates, it can be predicted that the resultant log DTP concentration time-profiles should exhibit three separate phases, that is, be sigmoidal. From the dose ranging studies it was observed that the decline of DTP blood concentration did in fact occur in three distinct phases, according to the dose administered. However it is evident, that the time course of the higher dose disposition study was insufficient to observe the three phases within a single experiment. Consequently, the DTP 10mg/kg single dose study was repeated, with sampling over a 250 hour period, measuring blood concentration decline over four orders of magnitude (see Fig. 6). This study verified the three phase, sigmoid profile behaviour. In the initial phase (concentration above 1mg/L) there is saturation of the DTP N-dealkylation metabolic route in conjunction with saturation of the high affinity hepatic DTP binding process due to high azole concentrations. The more rapid decline of the second phase (concentrations between 0.05–1mg/L) can be attributed to the linearization of metabolic clearance whilst the liver binding remains essentially saturated, and the third phase (0.05mg/L) can be termed the linear phase where both the metabolism and liver binding proceed under first order conditions.

Comparing the Km (based on unbound blood concentrations) and Kd estimates reveals that the cytochrome P450 isoforms involved in the metabolism of DTP have lower affinity for DTP than the liver binding sites. The nature of the liver binding sites is essentially unknown, however, spectral binding studies demonstrate that hepatic microsomal cytochromes P450 exhibit a strong affinity for DTP. The *in vitro* dissociation constant is similar in value to the *in vivo* Kd. Furthermore, a value of 50nmol cytochromes P450/g liver has been recorded for rats in our laboratory (D. Carlile, unpublished) and the maximum capacity of the saturable binding component was estimated to be 12nmol/g liver. Thus it is feasible that a proportion of the saturable liver binding sites may involve particular cytochromes P450. However it is also evident that DTP must bind to cytochrome P450 isoforms which do not have the ability to metabolize it. This phenomenon is not unprecedented. Quinidine has been reported to bind, two orders of magnitude, more avidly to cytochromes P450IID than to cytochrome P450IIIA3. The latter isoform is the major enzyme involved in the oxidation of quinidine, whereas the former isoform does not oxidize it at all (29).

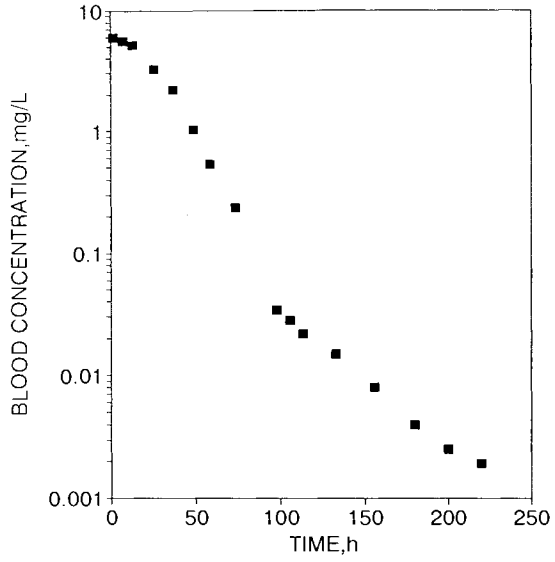

Figure 6. Blood concentration-time profile for DTP following bolus administration of 10mg/kg with sampling over 10 days.

In conclusion, both ketoconazole and DTP display similar behaviour in microsomes, however, DTP has several advantages over ketoconazole *in vivo*. Furthermore to our knowledge DTP is the first example of a strong positive dependence of V upon drug binding in the liver. The impact of this distribution phenomenon together with the nonlinear metabolism of DTP leads to the sigmoidal log concentration-time profile following administration of a high dose of DTP.

ACKNOWLEDGEMENTS

Financial support from the Science and Engineering Research Council is gratefully acknowledged in the form of a CASE award with Pfizer Central Research, Sandwich, Kent, UK.

REFERENCES

1. D. R. Kirsch, M, H. Lai and J. O'Sullivan. Isolation of the gene for cytochrome P450L1A1 (lanosterol 14α-demethylase) from *Candida albicans*. *Gene* 68:229–237 (1988).
2. Y. Yoshida and Y. Aoyama. Interaction of azole fungicides with yeast cytochrome P450 which catalyzes lanosterol 14α-demethylation. In: *In vitro* and *In vivo* Evaluation of Antifungal Agents. K. Iawata and H. Van den Bossche (Eds.) Elsevier, Amsterdam, pp. 123–134 1986.
3. P. R. Ortiz de Montellano and N. O. Reich. Inhibition of cytochrome P450 enzymes. In: Cytochrome P450, Structure, Mechanism and Biochemistry. P. R. Ortiz de Montellano (Ed.) Plenum Press, London, pp. 273–314 (1986).
4. J. J. Sheets and J. I. Mason. Ketoconazole—a potent inhibitor of cytochrome P450 dependent drug metabolism in rat liver. *Drug Metab. Dispos.* 12:603–606 (1984).
5. M. Pasanen, T. Taskinen, M. Iscon, E. A. Sonaniemi, M. Kairaluma and O. Pelkonen. Inhibition of human hepatic and placental xenobiotic monooxygenases by imidazole antimycotics. *Biochem. Pharmacol.* 37:3861–3866 (1988).
6. K. Lavrijsen, J. Van Houdt, D. Thijs, W. Meuldermans and J. Heykants. Interaction of miconazole, ketoconazole and intraconazole with rat liver microsomes. *Xenobiotica* 17:45–57 (1987).
7. P. Mosca, P. Bonzzi, G. Novelli, A. M. Jezequel and F. Orlandi. *In vitro* inhibition of hepatic microsomal drug metabolism by ketoconazole. *Br. J. Exp. Pathol.* 66:737–742 (1985).
8. C. G. Meredith, A. L. Maldonado and K. V. Speeg. The effect of ketoconazole on hepatic oxidative drug metabolism in the rat *n vivo* and *in vitro*. *Drug Metab. Dispos.* 13:156–162 (1985).
9. J. B. Houston, M. J. Humphrey, D. E. Matthew and M. H. Tarbit. Comparison of two azole antifungal drugs, ketoconazole

and fluconazole, as modifiers of rat hepatic monooxygenase activity. *Biochem. Pharmac.* 37:401–408 (1988).
10. R. G. Thompson, M. D. Rawlins, O. F. W. Jones, P. Wood and F. M. Williams. The acute and subchronic effects of ketoconazole on hepatic microsomal monooxygenases in the rat. *Biochem. Pharmac.* 37:3975–3980 (1988).
11. D. Matthew, B. Brennan, K. Zomorodi and J. B. Houston. Disposition of azole antifungal agents I. Nonlinearities in ketoconazole clearance and binding in rat liver. *Pharm. Res.* 10:418–422 (1993).
12. R. P. Remmel, K. Amoh, and M. M. Abdel-Monem. The disposition and pharmacokinetics of ketoconazole in the rat. *Drug Metab. Dispos.* 15:735–739 (1987).
13. J. B. Houston. Drug metabolite kinetics. *Pharm. Therap.* 15:521–552 (1982).
14. H-S. G. Chen and J. F. Gross. Estimation of tissue-to-plasma partition coefficients used in physiological pharmacokinetic models. *J. Pharmacokin. Biopharm.* 7:117–125 (1979).
15. J. R. Gillette. Factors affecting drug metabolism. *Ann. N.Y. Acad. Sci.* 179:43–66 (1971).
16. J. B. Schenkman, H. Remmer and R. W. Estabrook. Spectral studies of drug interactions with hepatic microsomal cytochrome. *Mol. Pharmac.* 3:117–123 (1967).
17. R. A. Prough, M. D. Burke and R. T. Mayer. Direct fluorometric methods for measuring mixed function oxidase activity. In: Methods in Enzymology, LII, Biomembrones, Part C. S. Fleischer and L. Packer (Eds.). Academic Press, London. pp. 372–377 (1978).
18. B. M. Brenner, W. M. Deen and C. R. Robertson. Glomerular filtration. In: *The Kidney*. B. M. Brenner and F. C. Rector (Eds.) W. B. Saunders, Eastbourne, UK, pp. 251–271 (1981).
19. Y. Yoshida and Y. Aoyama. Interaction of azole antifungal agents with cytochrome P-450$_{14DM}$ purified from *Saccharomyces cerevisiae* microsomes. *Biochem. Pharmac.* 36:229–235 (1987).
20. A. D. Rodrigues, G. G. Gibson, C. Ioannides and D. V. Parke. Interactions of imidazole antifungal agents with purified cytochrome P450 proteins. *Biochem. Pharmac.* 36:4277–4281 (1987).
21. T. L. Poulos. Cytochrome P450: molecular architecture, mechanism and prospects of rational inhibitor design. *Pharm. Res.* 5:67–75 (1988).
22. W. K. Cheung and G. Levy. Comparative pharmcokinetics of coumarin anticoagulants XLIX: Nonliner tissue distribution of S-warfarin in rats. *J. Pharm. Sci.* 78:541–546 (1989).
23. D. Trenk, B. Winkelmann, E. Jahnchen and S. Oie. Dose dependent metabolism and hepatic distribution of phenprocoumon in rats. *J. Pharmacokin. Biopharm.* 16:1–12 (1988).
24. S. A. Ballard, A. Lodola and M. Tarbit. A comparative study of 1-substituted imidazole and 1,2,4-triazole antifungal compounds as inhibitors of testosterone hydroxylations catalysed by mouse hepatic microsomal cytochromes P450. *Biochem. Pharmac.* 37:4643–4651 (1988).
25. G. R. Wilkinson. Clearance approaches in pharmacology. 39:1–47 (1987).
26. S. Oie and T. N. Tozer. Effect of altered plasma protein binding on apparent volume of distribution. *J. Pharm. Sci.* 68:1203–1205 (1979).
27. C. A. M. Van Ginnekan, J. M. Van Rossum and H. L. J. M. Fleuren. Linear and nonlinear kinetics of drug elimination I. Kinetics on the basis of a single capacity-limited pathway of elimination with or without simultaneous supply-limited elimination. *J. Pharmacokin. Biopharm.* 2: 395–415 (1974).
28. S. Oie, T. W. Guentert and T. N. Tozer. Effect of saturable binding on the pharmacokinetics of drugs: A simulation. *J. Pharm. Pharmac.* 32:471–477 (1980).
29. F. P. Guengerich, D. Muller-Enoch and I. A. Blair. Oxidation of quinidine by human liver cytochrome P450. *Mol. Pharmac.* 30:287–295 (1987).